Proceedings of Ninth World Conference on Earthquake Engineering
August 2-9, 1988, Tokyo-Kyoto, JAPAN (Vol.II)

3-3-8

ESTIMATION OF STRONG GROUND MOTION IN THE TOKYO METROPOLITAN AREA DURING THE 1923 GREAT KANTO EARTHQUAKE

Etsuzo SHIMA[1], Manabu KOMIYA[2] and Keiji TONOUCHI[3]

[1]Professor Emeritus, University of Tokyo, Tokyo, Japan
[2]Japan Metrological Agency, Tokyo, Japan
[3]Oyo Corporation, Tokyo, Japan

SUMMARY

This paper concerns an attempt to estimate in detail the distribution of seismic motion, which is a basic parameter in microzonation, that occurred during the most destructive earthquake in Japan's history, the 1923 Kanto Earthquake. The investigation covers the greater Tokyo metropolitan area, which constitutes the hub of Japan's political, economic and cultural activities. When the J.M.A. seismic intensity scale is divided into two ranks, comparison with seismic intensities calculated from actual damage shows that approximately 90% of the results fall within a range of one rank.

INTRODUCTION

Seismic microzonation is a very effective method for planning countermeasures against earthquake disasters. Seismic microzonation specifies unit areas and evaluates the risk of earthquakes, the area's characteristics for the purpose of forcasting earthquake damage. The process is presupposed on evaluation of seismic motion on the ground surface, which is an important factor determining results. The greater metropolitan area of Japan's capital city of Tokyo, which includes neighboring prefectures, constitutes the center of political and economic activity. The population in this area has been increased up to a quarter of Japan's total inhabitants. The 1923 Kanto Earthquake brought severe damage to Tokyo and its environs. Since the earthquakes occur repeatedly at the same origin, the advancement of earthquake disaster countermeasures in this area is highly desirable.

Using data on damage from the 1923 Kanto Earthquake and taking into consideration the vibration characteristics of the subsurface layers, the capital area was divided into squares approximately 1 kilometer on a side, ground surface seismic motion was evaluated. The method proposed in this paper is explained in Fig. 1.

GROUND CLASSIFICATION

Ground classification was conducted in two stages, as shown in Fig. 2. First, using the existing information on the objective area of this study, ground types were classified according to geology and layer thickness, as the primary classification of topographical and geological characteristics. 120 ground types were identified from an objective area. Models of each ground type were constructed by assigning S-wave velocity, density and damping coefficients. Transfer function for each model was calculated by the SH-wave multiple reflection method. Then, reclassification was conducted by combining ground types showing similar locations of first peaks and amplification ratios of transfer functions, so that 20 ground types were settled upon.

The amplification characteristics during an earthquake of each of the final 20 ground types thus obtained were determined. Using actual earthquake waveform records, and on the basis of SH-wave multiple reflection theory, response analysis of the horizontally parallel layer structure was conducted, taking into account the non-linearity of the soil. The waveform used in calculation was the one observed during the 1968 Tokachi-Oki Earthquake ($M = 7.9$) approximately 180 km away from the epicenter, at Hachinohe Harbor. Before the data was input, the effects of the subsurface layers at the observation point were eliminated. Several incident acceleration values were assigned each model to calculate ground surface response acceleration. From these results, an amplification curves expressing the relationship between horizontal axis incidental acceleration and vertical axis surface acceleration was created.

Evaluation of ground surface seismic motion was conducted at each mesh consisting of squares approximately 1 km on a side. However, when excluding the area of mountains and table land, we often find several ground types mixed together. One method of using one representative ground type to one square is shown in Fig. 3. By this method, the predominant ground type is determined. Fig. 4 shows an example of ground classification by the above method. The distinction was made on the basis of soil type of the top layer.

ACCELERATION AT THE BASE LAYER

Data on damage from the 1923 Kanto Earthquake was used in determining incidental acceleration to the base layer. A great deal of useful information on this is available. Since wooden houses were the most common structures in Japan, the rate of damage to wooden houses has long been used as standard for comparing seismic motion by regions. Therefore, using these data, we converted data on damage to wooden houses to acceleration values, adopting Mononobe's formula (1926) to express the relationship between rate of totally collapsed wooden houses and seismic intensity. This method was applied to convert the rate of totally collapsed wooden houses per administrative district to acceleration values, using maps of the period, to obtain Fig. 5. This figure shows ground surface acceleration values for each village and town.

Next from these ground surface acceleration values, the previously determined amplification curves for different ground types were used to eliminate amplification of subsurface and determine acceleration values at the base layer, which corresponds to the layer having the shear wave velocity of approximately 500 m/s. According to Fig. 7, correction between different base layers were made. Fig. 6 express the relationship between acceleration value and distance from the fault plane by Kanamori and Ando's model (1973). The white circles in the figure indicate acceleration values at the base layer. While the black dots in the figure indicate acceleration values at the ground surface. The equation in the figure shoes how incidental acceleration at the base layer attenuates with distance from the fault plane.

ESTIMATION OF ACCELERATION

Ground surface acceleration was determined using the data on incidental acceleration at the base layer, ground type, and amplification of the subsurface of each square. This is expressed in Fig. 8 in increments of 50 gals. Comparing these results with the ground classifications in Fig. 4, we see that acceleration values are high in the lowland soft ground areas of the Tokyo Bay coast, while in the rock zone at the left (west) of the figure, acceleration values are low. Acceleration levels correspond well with ground conditions.

Seismic intensities below VI are divided into two ranks. Fig. 9 is a histograph showing seismic intensity rank differential. From this, approximately 40% of data correspond completely to seismic intensity rank. When a differential of 1 rank is allowed, correspondence of 90% is obtained.

CONCLUSIONS

The method for estimating seismic motion in Tokyo Metropolitan area during the 1923 Great Kanto Earthquake was presented. Through the study, we could infer the seismic motion successfully at the sites where no observed data is available at the period. When the J.M.A. seismic intensity scale is divided into two ranks, comparison with seismic intensities from actual damage shows that approximately 90% of the results fall within a range of 1 rank. Usually, subsurface ground condition in Japan is complex. We found sometimes several ground types in a mesh. So the smaller the mesh size, higher will be the accuracy of estimation.

REFERENCES

1. Tsuchida,H., E.Kurata, K.Sudo (1969): Strong Motion Earthquake Records on the 1968 Tokachi-Oki Earthquake and Its aftershocks, Technical Note of the Port and Harbor Research Institute, Ministry of Transport, Japan, No.80.
2. Ministry of Interior, Japan (1925): Taisho Shinsai-Shi (Memorial of Taisho Great Disastrous Earthquake).
3. Matsuzawa,T. (1925): Intensity Distribution Deduced from the Damage on Wooden Buildings, Reports of the Imperial Earthquake Investigation Committee, No.100, D.
4. Mononobe,N. (1926): General Reports on the Damage to Public Civil Engineering Works Caused by the Great Earthquake, Reports of the Imperial Earthquake Investigation Committee, No.100, A.
5. Kanamori,H., M.Ando (1973): Fault Parameters of the Great Kanto Earthquake of 1923, Publication for the 50th Anniversary of the Great Kanto Earthquake, 1923.

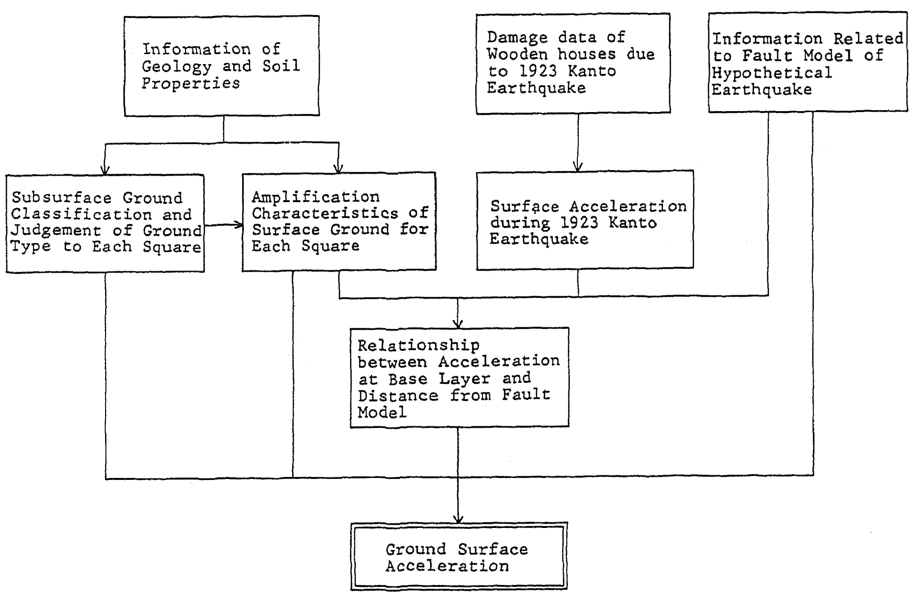

Fig. 1 Flowchart for estimating surface ground motion during earthquake

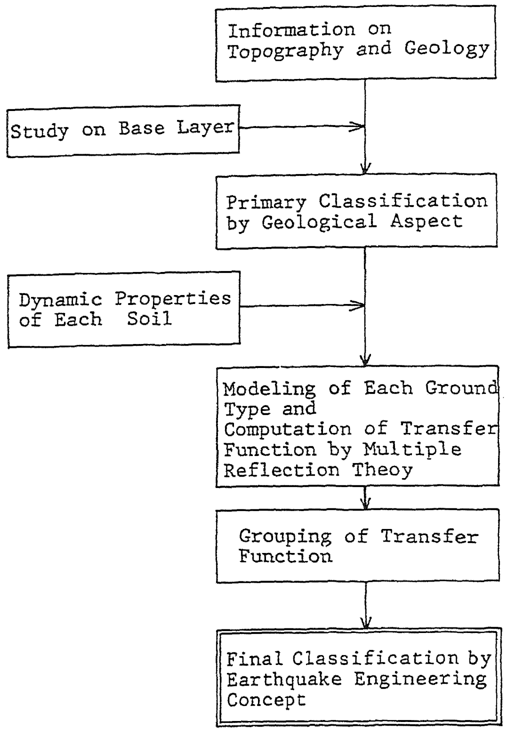

Fig. 2 Basic scheme for Ground classification

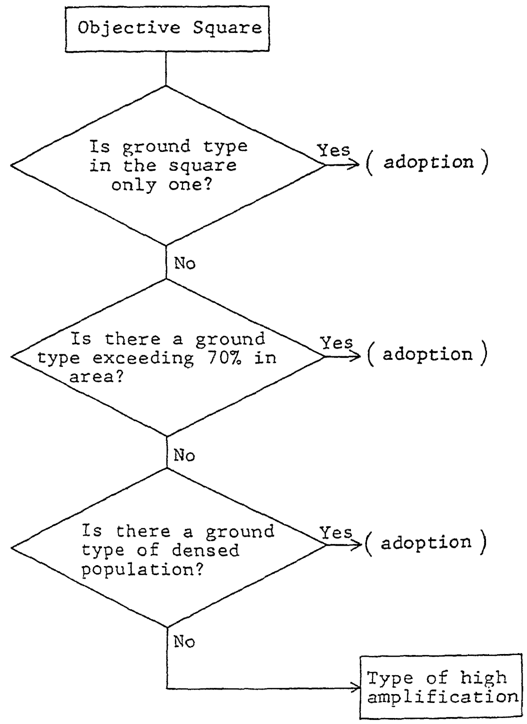

Fig. 3 Procedure for judgement of representative ground type for each square

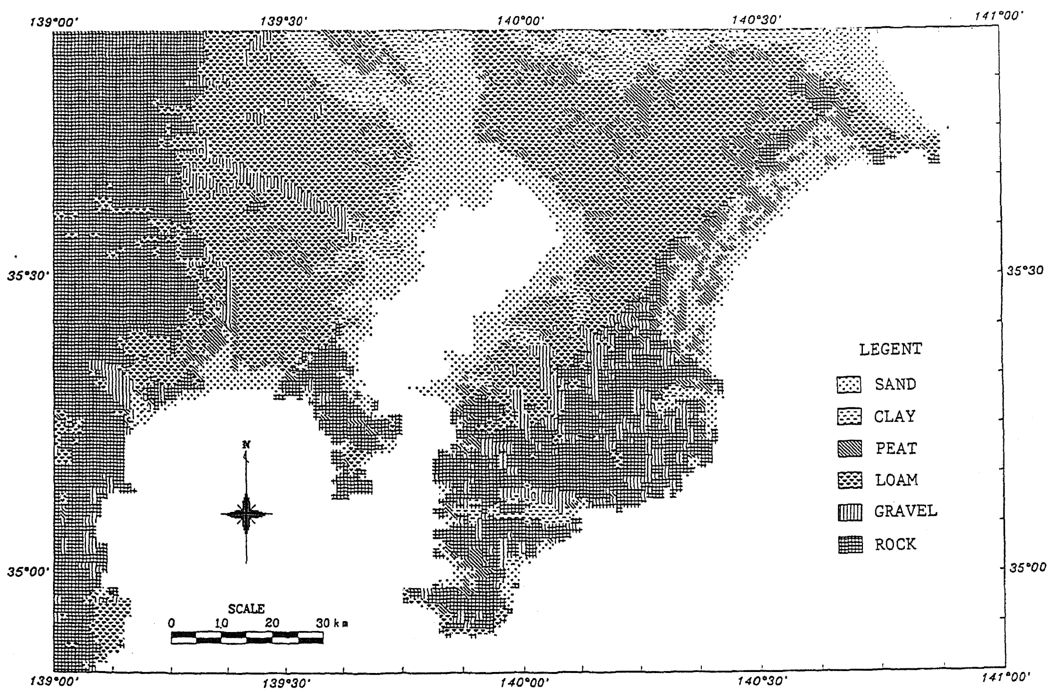

Fig. 4 Subsurface geological map

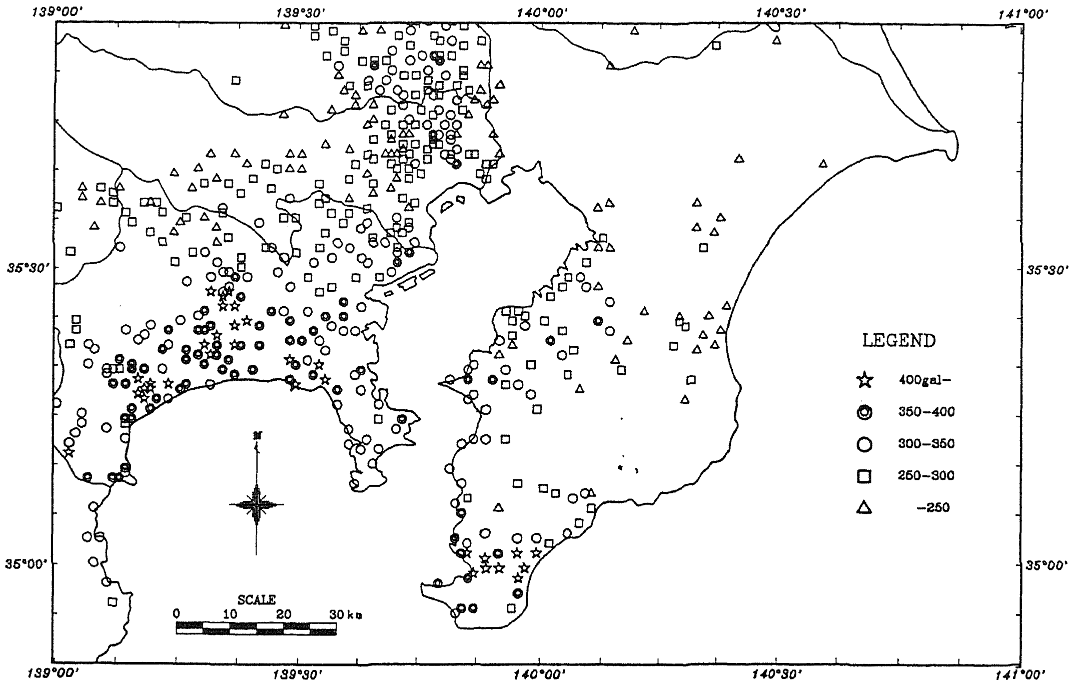

Fig. 5 Surface acceleration estimated from damage of wooden houses due to 1923 Kanto Earthquake

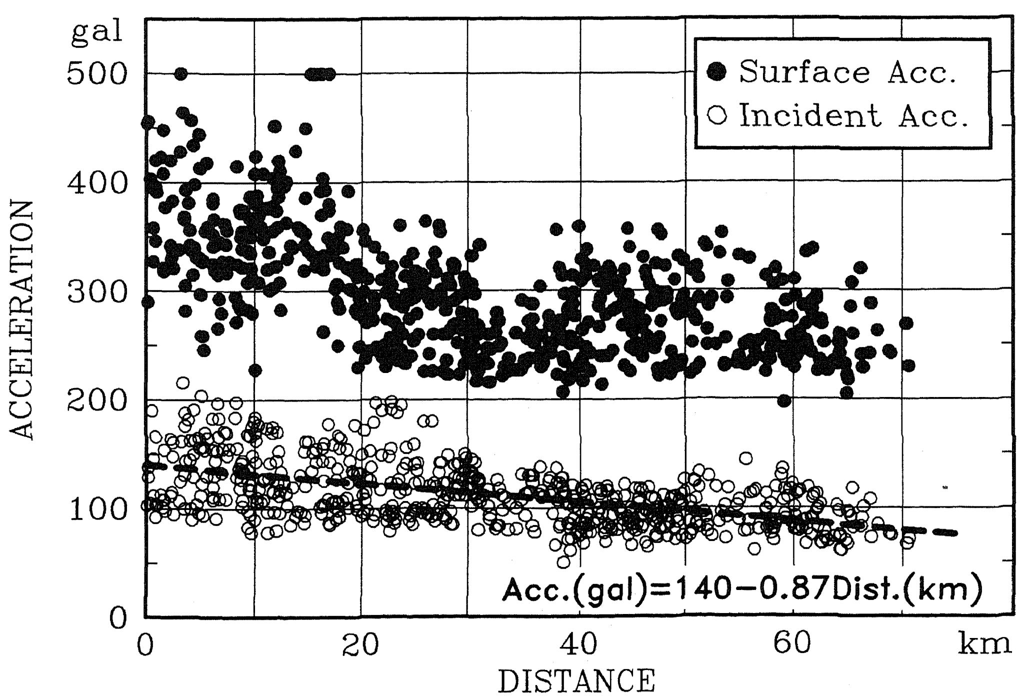

Fig. 7 Surface and incident acceleration due to 1923 Kanto Earthquake estimated from damage data and surface ground amplification

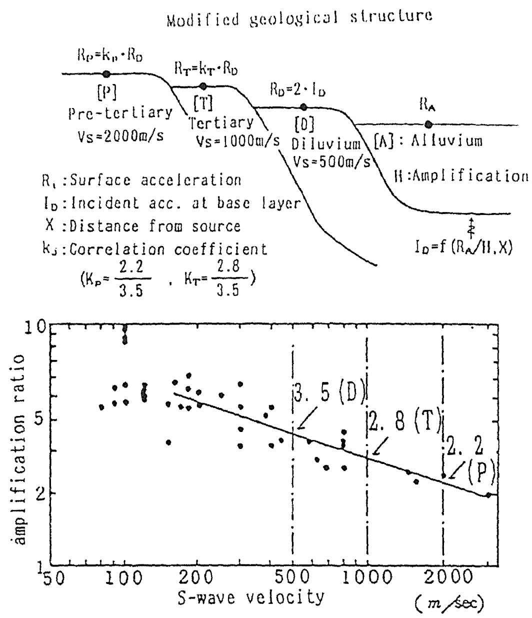

Relation between S-wave velocity of surface and amplification ratio [Midorikawa (1980)]

Fig. 6 Modified geological structure and correlation of acceleration at the base layers

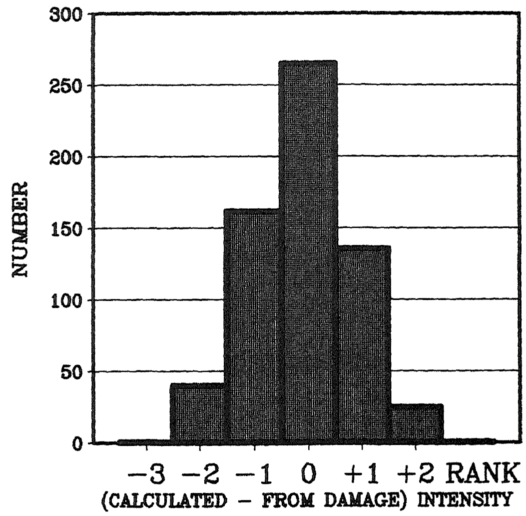

Fig. 9 Histograph of seismic intensity differential between calculated and estimated from damage

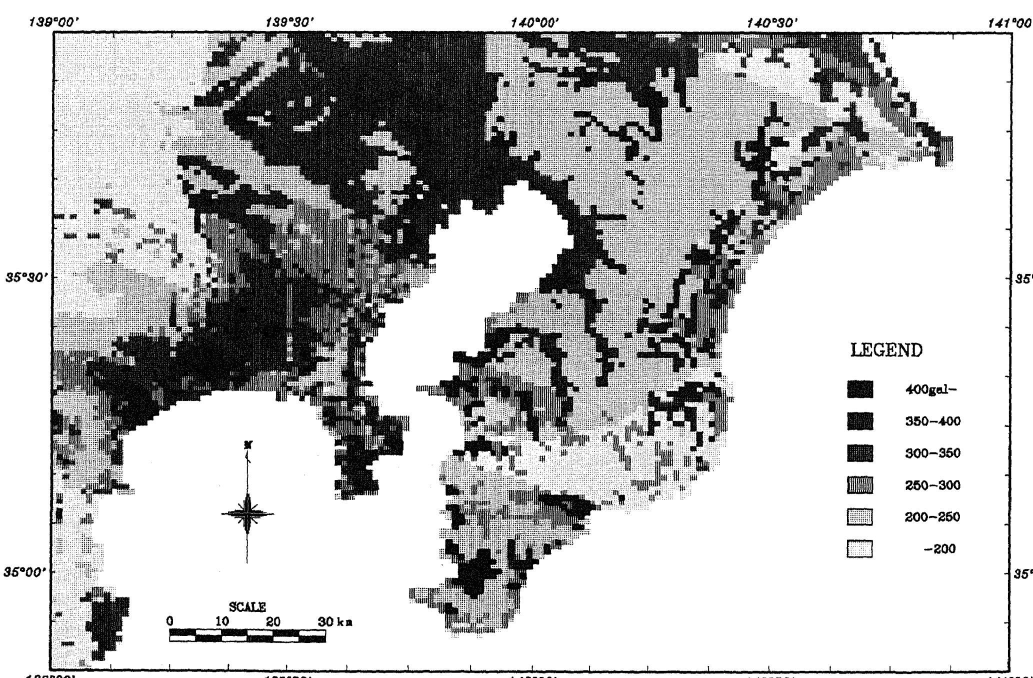

Fig. 8 Surface acceleration map calculated for 1923 Kanto Earthquake